



**HAL**  
open science

## Colored electrolytes for electrochromic devices

Cyril Périé, Valentin Mary, Brandon Faceira, Aline Rougier

► **To cite this version:**

Cyril Périé, Valentin Mary, Brandon Faceira, Aline Rougier. Colored electrolytes for electrochromic devices. *Solar Energy Materials and Solar Cells*, 2022, 238, pp.111626. 10.1016/j.solmat.2022.111626 . hal-03562001

**HAL Id: hal-03562001**

**<https://hal.science/hal-03562001>**

Submitted on 8 Feb 2022

**HAL** is a multi-disciplinary open access archive for the deposit and dissemination of scientific research documents, whether they are published or not. The documents may come from teaching and research institutions in France or abroad, or from public or private research centers.

L'archive ouverte pluridisciplinaire **HAL**, est destinée au dépôt et à la diffusion de documents scientifiques de niveau recherche, publiés ou non, émanant des établissements d'enseignement et de recherche français ou étrangers, des laboratoires publics ou privés.

# Colored Electrolytes for Electrochromic Devices

Cyril Périé, Valentin Mary, Brandon Faceira and Aline Rougier\*

*Université de Bordeaux, CNRS, Bx INP, ICMCB-UMR 5026, F-33600 Pessac, France.*

- Corresponding author : [aline.rougier@icmcb.cnrs.fr](mailto:aline.rougier@icmcb.cnrs.fr)

**Abstract:** Color tuning remains one of the main issues for electrochromic applications. Multicolored organic and inorganic electrochromic materials have been largely studied. Herein, a novel approach of color modulation is investigated : the electrolyte coloration. The color tuning is therefore not only due to electrochromic materials but addressed thanks to pigment addition in the electrolyte, which allows endless possibilities. A symmetrical PEDOT:PSS based display and a  $\text{WO}_3/\text{V}_2\text{O}_5$  display were elaborated in order to characterize this coloration process. The PEGDMA/PEGMA copolymer gel electrolyte was processed by thermal polymerization using AIBN and colored using four different pigments. Similar switching times and capacities were measured from one colored electrolyte to another. This easy to set up method multiplies the achievable colors without altering electrochromic device stability.

**Keywords:** Electrochromic, display, electrolyte, PEDOT:PSS, color-tuning, colorimetry

## 1. Introduction

Electrochromic devices, ECDs, are defined as systems that can reversibly change their optical properties in response to an applied voltage [1]. ECDs received growing interests in many applications such as smart windows, rearview mirrors and displays [2–6]. One main challenge of this research field is to achieve a large color palette to diversify its applications, especially for displays. Literature demonstrates multicolored properties of inorganic electrochromic displays based on  $\text{WO}_3$  and  $\text{V}_2\text{O}_5$  [7–9]. Color tuning is also obtained with electrochromic polymer materials by changing the polymer chain (e.g., carbazole, thiophene or pyrrole based polymer) or by group substitution [10–12]. Our previous works intro-

duce another way of color modulation by adding pigments in the electrochromic poly(3,4-ethylenedioxythiophene, polystyrene sulfonate, PEDOT:PSS layer [13–15]. Herein, we investigate a new method to tune the color of electrochromic displays by changing the color of the electrolyte. Four pigments (three oxides and a blend of small molecules) are mixed to a gel polymer electrolyte in order to propose four different colors.

Polymer based electrolytes are classified in several types [16]. Among them, solid-state polymer electrolytes are solvent free systems with an ionic conducting phase formed by dissolved salt [17,18]. Studies have demonstrated the enhancement of the ionic conductivity of solid-state polymer electrolyte with the addition of oxide particles such as,  $\text{Al}_2\text{O}_3$ ,  $\text{TiO}_2$ ,  $\text{SiO}_2$  [19–21]. Adding oxides favors the formation of an amorphous phase of the polymer, increases the glass transition temperature and enhances the conductivity [20,22]. Furthermore, an improvement of the electrode/electrolyte interface stability due to oxide particles has been reported [23,24]. Then, gel polymer electrolytes are usually obtained by incorporating a larger quantity of ionic liquid or solvent/salt to a polymer matrix that is capable of forming a stable gel [25,26]. An enhancement of the ionic conductivity and of the cycling stability has also been mentioned with the addition of oxide particles in gel polymer electrolytes [27–29]. Besides, gel polymer electrolytes exhibit a higher ionic conductivity compared to solid-state electrolytes.

The polymer network of the gel electrolyte used in this study is formed of two oligomers, the polyethylene glycol dimethacrylate (PEGDMA) and the polyethylene glycol methacrylate (PEGMA). This copolymer is already used in electrochromic devices, lithium batteries and actuators [30–33]. Liu et al reported the impact of  $\text{SiO}_2$  nanoparticles on the ionic conductivity of gel electrolyte based on PEGMA PEGDMA polymer network [22]. They concluded that the  $\text{SiO}_2$  nanoparticles did not enhance the conductivity of the electrolyte because the polymer network presents a fully amorphous state. Thereby, this polymer network seems to be a good choice to change the electrolyte color without modifying the ionic conductivity. The PEGMA / PEGDMA can be polymerized with a thermal or a UV crosslinker [30,32]. Oxide particles used in this study such as  $\text{TiO}_2$  or  $\text{Fe}_2\text{O}_3$  are absorbent in the UV range [34–36]. Then thermal activation is a more appropriate way to get a complete and homogeneous polymerization. Firstly, colored electrolytes are integrated to symmetrical PEDOT:PSS based displays which is easy to process.

Then an inorganic display, based on  $\text{WO}_3/\text{V}_2\text{O}_5$  electrochromic materials, with four different electrolyte colors is presented.

## 2. Materials and Methods

### 2.1 Gel polymer electrolyte formulation

The thermal initiator Azobisisobutyronitrile (AIBN), the texturizing agent Polyethylene glycol (PEG,  $M_n$  35000 g.mol<sup>-1</sup>), the copolymer precursors polyethylene glycol dimethacrylate (PEGDMA) and polyethylene glycol methacrylate (PEGMA) were purchased from Sigma-Aldrich. The ionic liquid Lithium bis(trifluoromethanesulfonyl)imide in 1-Ethyl-3-methylimidazolium bis(trifluoromethylsulfonyl)imide (LiTFSI : EmimTFSI (1:9 molar ratio)) was purchased from Solvionic. AIBN was recrystallized in methanol before use. The PEG, PEGMA, PEGDMA and the ionic liquid were mixed with a weight ratio of 1 : 6 : 1 : 12 and stirred at 80 °C for 2 hours until PEG is completely dissolved. When the formulation was cooled down at room temperature, AIBN was added (4.5 wt% compared to the PEGDMA + PEGMA weight). Then, the resulting preparation was stirred at room temperature for overnight.

For the electrolyte coloration, four different pigments were chosen. Jaune 920 (yellow), Rouge 110 (red) and Vert 4FR (green), respectively composed of iron oxyhydroxide ( $\text{FeOOH}$ ), hematite ( $\alpha\text{-Fe}_2\text{O}_3$ ) and a blend of copper phthalocyanine ( $\text{C}_{32}\text{H}_{16}\text{CuN}_8$ ) and monoazo pyrazolone ( $\text{C}_{16}\text{H}_{12}\text{C}_{12}\text{N}_4\text{O}$ ), were purchased from Ogres de France.  $\text{TiO}_2$  (white) was purchased from Sigma-Aldrich. They were added to the gel polymer electrolyte formulation and stirred at room temperature for 4 hours.

### 2.2 Symmetrical PEDOT:PSS based display processing

The electrochromic ink was prepared from commercial PEDOT:PSS ink Afga Orgacon EL-P5015 (called hereinafter PEDOT:PSS). The formulation was prepared mixing 60 wt% of PEDOT:PSS paste and 40 wt% of ethanol. The solution was stirred for 5 min at room temperature, then dispersed using an ultrasonic bath for 30 min and stirred again for 5 min.

For the electrolyte coloration, four formulations were prepared. 10 wt%  $\text{TiO}_2$ , 5 wt% Jaune 920, 5 wt% Rouge 110 + 5 wt%  $\text{TiO}_2$  and 5 wt% Vert 4FR + 5 wt%  $\text{TiO}_2$  were added to the electrolyte base

to obtain the white, yellow, red and green colors, respectively. To get a fully opaque electrolyte, red and green pigments are mixed with TiO<sub>2</sub>.

The displays were built in a symmetric configuration. For each device the same process was employed on two substrates before assembly. PEDOT:PSS ink was deposited on two ITO-coated (In<sub>2</sub>O<sub>3</sub>:Sn) glass substrates (commercialized by Solems with a resistance of 30 Ω □<sup>-1</sup>) with a bar coater and dried at 120 °C for 10 min on a hot plate (1 μm thick was obtained). Two adhesive tape bands (60 μm thick, 2 mm wide) were placed all along the sides of the two PEDOT:PSS/ITO/glass electrodes. The gel polymer electrolyte formulation was then deposited by bar coater on both PEDOT:PSS/ITO/glass electrodes. The two pieces were assembled and placed on a hot plate for 10 min at 50 °C to obtain a homogeneous polymerization. The obtained average thickness for the electrolytic membrane was 120 μm ± 10 μm. The final stack for each symmetrical PEDOT:PSS based display presented in this article is glass / PEDOT:PSS / (EmimTFSI : LiTFSI + copolymer + pigments) / PEDOT:PSS / ITO / glass.

### *2.3 Multi-colored WO<sub>3</sub>/electrolyte/Li<sub>x</sub>V<sub>2</sub>O<sub>5</sub> display processing*

The ITO coated glass substrates were ultrasonically cleaned with ethanol and distilled water before being introduced in the chamber. WO<sub>3</sub> and V<sub>2</sub>O<sub>5</sub> films were prepared by radiofrequency magnetron sputtering in a PLAYSSIS MP700 apparatus using WO<sub>3</sub> and V targets (99.9% purity) purchased from Neyco of 75 mm of diameter and 3 mm thick. Prior to the deposition process, the base pressure in the chamber was set below 3.10<sup>-7</sup> mbar. The target to substrate distance was set at 10 cm. Deposition parameters are detailed in table 1. Prior to deposition, a plasma stabilization step of 20 min was done with a shutter, then the shutter was open to allow deposition. The films were grown without intentional substrate heating. At the end of sputtering, the WO<sub>3</sub> target was reoxidized in a 10% O<sub>2</sub> plasma atmosphere and the vanadium one was reduced in argon atmosphere. Films thickness was determined by mechanical profilometry using a Dektak instrument.

For the electrolyte coloration, four formulations were prepared with different pigments. 10 wt% TiO<sub>2</sub>, 0.5 wt% Jaune 920 + 10wt % TiO<sub>2</sub>, 0.25 wt% Rouge 110 + 10 wt% TiO<sub>2</sub> and 2 wt% Vert 4FR + 10 wt% TiO<sub>2</sub> were added to the electrolyte base to obtain the white, yellow, red and green colors, respectively.

Before being incorporated in display, insertion of lithium in  $V_2O_5$  electrode was performed by chronoamperometry for 5 minutes in LiTFSI:EmimTFSI (1:9 mol) applying a potential of -0.9 V in 3-electrode cell using a Pt counter electrode and SCE reference electrode. For the multi-colored  $WO_3$ /electrolyte/ $Li_xV_2O_5$  ( $x \approx 1$ ) display assembly, two symmetrical cross shapes spacers made with adhesive tape (60  $\mu\text{m}$  thick, 2 mm wide) were placed in the centre of the  $WO_3$ /ITO/glass electrode and  $Li_xV_2O_5$ /ITO/glass electrode. White, yellow, red and green electrolytes were deposited on the  $WO_3$ /ITO/glass electrode with a bar coater while white electrolyte was deposited on the  $Li_xV_2O_5$ /ITO/glass electrode. The two pieces were assembled and placed on a hot plate for 10 min at 50  $^\circ\text{C}$  to achieve a homogeneous polymerization.

#### *2.4 Characterization*

Concerning the ionic conductivity measurement, the electrolyte formulation was sandwiched between two stainless steel blocking electrodes with tape spacers and placed on a hot plate for 10 min at 50  $^\circ\text{C}$ . Then, samples were stored on a hot plate at 40  $^\circ\text{C}$  for 30 min before measurement. Electrochemical impedance spectroscopy was performed using Biologic SP50 potentiostat in the frequency range from 100 KHz to 10 Hz with perturbation amplitude of 10 mV.

FT-IR measurements were performed on the different electrolytes to evaluate the progress of polymerization. Electrolytes were sandwiched between two  $CaF_2$  substrates and polymerized in the same conditions than described previously. Full FT-IR spectra were obtained using a spectrometer BRUKER EQUINOX 55.

Electrochemical analysis were performed on displays in a two-electrode configuration, using a Biologic potentiostat / galvanostat apparatus at room temperature. The operating voltage was controlled between -1.5 V and 1.5 V for chronoamperometry (CA) analysis. Colorimetric analysis were carried out using a Konica Minolta CM-700D spectrophotometer, allowing the direct determination of colorimetric parameters of the CIE ( $L^*a^*b^*$ ) color space.

### 3. Results and discussion

#### 3.1. Electrolyte characterization

The electrolyte composition (copolymer precursors PEGDMA, PEGMA; thermal initiator AIBN; texturizing agent PEG, and ionic liquid LiTFSI:EmimTFSI) has been optimized to get a fast thermal polymerization (10 min). Symmetrical PEDOT:PSS based devices were also fabricated to validate the composition by measuring the switching time and the electrochemical stability. This composition has been chosen to avoid the use of UV treatment, which can degrade the pigments. Moreover, the addition of PEG can be modulated in order to adjust the electrolyte viscosity before the polymerization. Thereby, this electrolyte is compatible with a large number of deposition technics.

Pigments were added to the electrolyte base to color it. For the white color, 10 wt% of  $\text{TiO}_2$  was added to ensure a good compromise between a sufficient opaque film and a minimum  $\text{TiO}_2$  amount. 5 wt% of the pigments responsible of the colors yellow, red and green were added to electrolyte base. Due to pigment aggregation during the thermal treatment, 5 wt% of  $\text{TiO}_2$  was added to the red and green electrolytes to get opaque electrolytes. The colored electrolytes were sandwiched between two glass substrates and placed on a hot plate at 50 °C for 10 min. The photographs and the chromaticity parameters of the electrolytes are presented in figure 1.

To characterize intrinsically the electrolytes, ionic conductivity was measured by electrochemical impedance spectroscopy. In order to have reproducible measurements, every samples were placed on a hot plate during 30 min at 40 °C before any measurement. On figure 2.a, a variation of titanium oxide ( $\text{TiO}_2$ ) quantity was studied from 0 to 50 wt% of the total electrolyte weight. A maximum value of 1.8 mS/cm<sup>2</sup> is measured at 40 °C with 10 wt% of  $\text{TiO}_2$ , that confirms the choice of adding this quantity to the electrolyte to achieve the white color. This improvement of ionic conductivity adding  $\text{TiO}_2$  was also found in literature [28]. A large quantity of 50 wt% of  $\text{TiO}_2$  is added to the electrolyte and ionic conductivity of 1mS/cm<sup>2</sup> was measured at 40 °C.  $\text{TiO}_2$  can be used in large quantity in the electrolyte without important consequences on the switching time and coloration rate of the electrochromic display. A similar result has already been demonstrated in previous works with 40 wt%  $\text{TiO}_2$  [7]. On figure 2.b,

the ionic conductivity was measured on electrolytes with the different previous formulations. Electrolyte conductivities were comprised between 1.2 and 1.8 mS/cm<sup>2</sup> at 40 °C. A slight decrease is observed for the yellow, red and green electrolyte (figure 2.b). To estimate the impact of the difference of ionic conductivity on electrochemical performance, symmetrical PEDOT:PSS based displays were characterized and results are presented in the next part.

FT-IR analysis were realized on different electrolytes to evaluate the influence of the pigments addition on the polymerization conversion (figure 3). During the radical polymerization, the C=O bond of the methacrylate group of PEGDMA and PEGMA is conserved, while the C=C bond is converted in a simple carbon bond. On the dotted curve, corresponding to the electrolyte without thermal treatment, the C=C peak appears at 1634 cm<sup>-1</sup>. For the other treated electrolytes, this peak is almost non existent and a polymerization with a high rate of conversion is deduced. Note that the C=O peak in the methacrylate group was slightly shifted toward a higher wavenumber, from 1716 to 1725 cm<sup>-1</sup>, implying an increased carbonyl bond strength due to the loss of conjugation between the olefin and carbonyl groups during UV curing, as is already substantiated in the literature [37,38]. Considering the C=C peak decrease and the C=O peak shift of the treated electrolytes, it can be concluded that the addition of pigments doesn't influence the polymerization conversion.

### *3.2. Integration in devices*

#### *3.2.1 PEDOT:PSS based devices*

To characterize electrochemically the displays, chronoamperograms (CA) were measured. An oxidizing potential of +1.5 V was applied for 30 s, and a reducing potential of -1.5 V was applied for 30 s, during 500 cycles. The 1<sup>st</sup> cycle and the 500<sup>th</sup> cycle are presented on figure 4.a and 4.b, respectively. A reference display without pigment in the electrolyte was characterized and named colorless. It should be noticed that the curve shapes are relatively similar between the 1<sup>st</sup> cycle and the 500<sup>th</sup> cycle. After 500 cycles, no electrochemical loss can be observed with those chronoamperograms. For the 500<sup>th</sup> cycle, the current density slightly tends to reach the abscissa axis faster than for the 1<sup>st</sup> cycle, meaning that there is an improvement in properties. No significant trend can be concluded from a colored electrolyte



to another. Minor differences of maximum peaks can be explained by the process conditions and slight differences in PEDOT:PSS layer.

Kinetic information can be extracted from chronoamperograms data. To compare the kinetics between the different colored electrolytes, an arbitrary method has been employed based on this formula :

$$\tau = t_{0.37} - t_{ini}$$

Where  $\tau$  represents the switching time,  $t_{0.37}$  is the time when the density reaches 37% of the maximal density and  $t_{ini}$  is the moment when the first potential is applied.  $\tau$  is assumed as a partial switching time. The value of 37 % has been chosen to draw a parralel with the time constant of capacitor charge/discharge. All characteristic times are presented in table 2. For all configurations, no significant differences of characteristic times are observed between the 1<sup>st</sup> cycle and the 500<sup>th</sup> cycle, meaning that the stability is maintained for all colored electrolytes. Then, according to the switching characteristic time values, it can be concluded that the presence of the pigments in electrolyte does not change significantly the display switching time.

Figure 5 shows the coloration of the electrochromic displays based on PEDOT:PSS and the color of the electrolyte alone when it was sandwiched between two glass-substrates. Lighter colors are visible for the electrolyte alone, corresponding higher  $L^*$  values were measured (table 3). This is attributed to the PEDOT:PSS layer which is not completely transparent when it is oxidized. Indeed, the light blue color of the oxidized PEDOT:PSS can be observed on the white oxidized display photograph. Depending on the electrolyte, distinct colors are observed when devices are in their oxidized state and also when devices are in their reduced state. Nevertheless, the difference is more significant for oxidized displays. Then, the neutral state color is similar to the oxidized color. Herein, the displays reversibly return to their oxidized state when no potential is applied.

In order to complete the characterization, colorimetric measurement of  $L^*, a^*, b^*$  chromaticity parameters were carried out during CA measurements before and after 500 CA cycles. The optical contrast,  $\Delta E^*$  was then calculated from the  $L^*, a^*, b^*$  values using the following formula :

$$\Delta E^* = [(L^*_{\text{red}} - L^*_{\text{ox}})^2 + (a^*_{\text{red}} - a^*_{\text{ox}})^2 + (b^*_{\text{red}} - b^*_{\text{ox}})^2]^{1/2}$$

Here  $L^*_{\text{red}}$ ,  $a^*_{\text{red}}$  and  $b^*_{\text{red}}$  represent color state space parameters at the reduced state, and the  $L^*_{\text{ox}}$ ,  $a^*_{\text{ox}}$  and  $b^*_{\text{ox}}$  at the oxidized state. Chromaticity parameters and optical contrast are gathered in table 3. A slight decrease of the optical contrast is observed for the white electrolyte after 500 CA cycles. Moreover, optical contrast remains constant for the yellow, red and green electrolytes with slight increases for red and green. A significant difference of optical contrast is obtained for the displays with red and white electrolytes. This can be attributed to the difference of the  $L^*$  of the red and white electrolyte alone, lightly colored electrolyte induces a higher contrast.

To complete the stability study of the electrochromic displays, the percentage of capacity for the 1<sup>st</sup> cycle (100%) and for the 500<sup>th</sup> cycle are reported on figure 6. Capacities were calculated from the areas of the oxidative chronoamperograms presented on the figure 4. This way of representation is more suitable to detect capacity loss. In our case, for all colored electrolyte configurations, a drop of capacity is noticed. This is attributed to the fact that some zones on the displays edges are not switching after several hundred cycles. The centre of the display, where the colorimetric parameters were measured, does not seem to be affected at this stage of cycling. Nevertheless, a similar drop in between 15% to 20% of capacity is observed for the different electrolytes configurations. The evolution of capacity upon cycling as well as of the switching time allows to conclude that the addition of those pigments do not modify the displays behaviour, despite the slight differences of ionic conductivity presented on figure 2.b.

### 3.2.2 Oxide based devices

To illustrate a possible application of multicolored electrolytes, a display with four patterns colored by four different electrolytes was built. The idea, was to achieve a display with several patterns which can switch from the electrolyte color to a common color for all patterns. Tungsten trioxide ( $\text{WO}_3$ ) was used as working electrode and vanadium pentoxide with inserted lithium ( $\text{Li}_x\text{V}_2\text{O}_5$ ) as counter electrode. Photographs of the reduced and oxidized states of display are shown in figure 7. Compared to symmetrical PEDOT:PSS based displays, electrolytes were colored with a higher percentage of  $\text{TiO}_2$ . 10 wt% of  $\text{TiO}_2$  were added to all the electrolytes, then 0.5 wt% of pigment was added for the yellow

color, 0.25 wt% for the red and 2wt% for the green electrolyte. In that way, the opacity is conserved and the bleaching makes the electrolyte colors paler than the electrolyte used in PEDOT:PSS based displays. Herein, a similar dark blue covers all the different display patterns when the  $\text{WO}_3$  working electrode is reduced (figure 7.a). In agreement with the colorless  $\text{WO}_3$  sputtered layer, when it is oxidized, the  $\text{WO}_3$  electrode does not influence the apparent colors of the electrolytes (figure 7.b).

Colorimetric parameters were measured on the  $\text{WO}_3$ /electrolyte/ $\text{Li}_x\text{V}_2\text{O}_5$  display and presented in the table 4. Optical contrasts of each pattern were determined and comprised between 68.4 for the yellow pattern and 59 for the red pattern. Pattern with red electrolyte has the weaker contrast, as for the symmetrical PEDOT:PSS based device.

In table 5, optical contrasts were calculated from the optical parameters between each pattern for both reduced and oxidized displays. To illustrate these calculations, two contrasts are detailed. When the  $\text{WO}_3$  electrode is reduced, a contrast between the yellow pattern (figure 7.a bottom left pattern) and the white pattern (figure 7.a bottom right pattern) of 7.0 is calculated. Then, when the  $\text{WO}_3$  electrode is reduced, a contrast between the light pink pattern (figure 7.b top left pattern) and the light bluish-greenish pattern (figure 7.b top right pattern) of 16.2 is calculated. A mean contrast of 4.25 is found for the reduced display, which indicates a similar dark blue covering all the reduced display. Then, a mean contrast of 14.6 is calculated for the oxidized display, which indicates a good distinction of the different colors. One of the possible optimization would be to reduce contrasts between each pattern when  $\text{WO}_3$  is reduced while increasing the contrasts between each pattern when  $\text{WO}_3$  is oxidized.

#### **4. Conclusions**

A gel electrolyte based on a thermal polymerization was chosen to investigate multicolored electrolytes. Herein, an original approach of color modulation in electrochromic devices is presented. This electrolyte presents several advantages: it is solvent-free and easy to process without UV treatment. The electrolyte formulation was optimized to get a fast polymerization (10 min) while maintaining the display stability. Symmetrical PEDOT:PSS based displays were fabricated to evaluate the impact of the electrolyte coloration. No significant difference on display switching time and stability was detected between the colored and colorless electrolytes. Finally, four different colors of electrolytes were incorporated in displays with higher contrast based on the stacking  $\text{WO}_3/\text{electrolyte}/\text{Li}_x\text{V}_2\text{O}_5$ . Finally, by changing the pigment concentration, a colored and translucent electrolyte can be imagined and integrated in smart windows. Moreover it can also be used in batteries and dye sensitive solar cells.

**Acknowledgements** : The research presented here has been funded through the CELTIQUES project of Bordeaux University.

## References

1. Rai, V.; Singh, R.S.; Blackwood, D.J.; Zhili, D. A Review on Recent Advances in Electrochromic Devices: A Material Approach. *Adv. Eng. Mater.* 2020, 22, 2000082, doi:10.1002/adem.202000082.
2. Kim, J.-H.; Hong, J.; Han, S.-H. Optimized Physical Properties of Electrochromic Smart Windows to Reduce Cooling and Heating Loads of Office Buildings. *Sustainability* 2021, 13, 1815, doi:10.3390/su13041815.
3. Park, B.R.; Hong, J.; Choi, E.J.; Choi, Y.J.; Lee, C.; Moon, J.W. Improvement in Energy Performance of Building Envelope Incorporating Electrochromic Windows (ECWs). *Energies* 2019, 12, 1181, doi:10.3390/en12061181.
4. Ah, C.S.; Song, J.; Cho, S.M.; Kim, T.-Y.; Ryu, H.; Cheon, S.; Kim, S.; Kim, J.Y.; Kim, Y.-H.; Hwang, C.-S. Fabrication of Highly Transparent Electrochromic Mirror Device with Nanoporous Counter Electrode: Fabrication of High Transparent Electrochromic Mirror Device. *Bull. Korean Chem. Soc.* 2018, 39, 1186–1192, doi:10.1002/bkcs.11574.
5. Park, H.; Kim, D.S.; Hong, S.Y.; Kim, C.; Yun, J.Y.; Oh, S.Y.; Jin, S.W.; Jeong, Y.R.; Kim, G.T.; Ha, J.S. A Skin-Integrated Transparent and Stretchable Strain Sensor with Interactive Color-Changing Electrochromic Displays. *Nanoscale* 2017, 9, 7631–7640, doi:10.1039/C7NR02147J.
6. Wu, W.; Fang, H.; Ma, H.; Wu, L.; Wang, Q.; Wang, H. Self-Powered Rewritable Electrochromic Display Based on WO<sub>3-x</sub> Film with Mechanochemically Synthesized MoO<sub>3-y</sub> Nanosheets. *ACS Appl. Mater. Interfaces* 2021, acsami.1c01959, doi:10.1021/acsami.1c01959.
7. Mjejri, I.; Gaudon, M.; Rougier, A. Mo Addition for Improved Electrochromic Properties of V<sub>2</sub>O<sub>5</sub> Thick Films. *Solar Energy Materials and Solar Cells* 2019, 198, 19–25, doi:10.1016/j.solmat.2019.04.010.
8. Zhang, W.; Li, H.; Yu, W.W.; Elezzabi, A.Y. Transparent Inorganic Multicolour Displays Enabled by Zinc-Based Electrochromic Devices. *Light Sci Appl* 2020, 9, 121, doi:10.1038/s41377-020-00366-9.

9. Wang, L.; Guo, M.; Zhan, J.; Jiao, X.; Chen, D.; Wang, T. A New Design of an Electrochromic Energy Storage Device with High Capacity, Long Cycle Lifetime and Multicolor Display. *J. Mater. Chem. A* 2020, 8, 17098–17105, doi:10.1039/D0TA04824K.
10. Argun, A.A.; Aubert, P.-H.; Thompson, B.C.; Schwendeman, I.; Gaupp, C.L.; Hwang, J.; Pinto, N.J.; Tanner, D.B.; MacDiarmid, A.G.; Reynolds, J.R. Multicolored Electrochromism in Polymers: Structures and Devices. *Chem. Mater.* 2004, 16, 4401–4412, doi:10.1021/cm049669l.
11. Yuh-Shan Su; Tzi-Yi Wu Three Carbazole-Based Polymers as Potential Anodically Coloring Materials for High-Contrast Electrochromic Devices. *Polymers* 2017, 9, 284, doi:10.3390/polym9070284.
12. Kong, L.; Wang, M.; Ju, X.; Zhao, J.; Zhang, Y.; Xie, Y. The Availability of Neutral Cyan, Green, Blue and Purple Colors from Simple D–A Type Polymers with Commercially Available Thiophene Derivatives as the Donor Units. *Polymers* 2017, 9, 656, doi:10.3390/polym9120656.
13. Mjejri, I.; Rougier, A. PEDOT:PSS/Fe<sub>2</sub>O<sub>3</sub> as Hybrid Composite Film for Tuning Color in Electrochromism. *Materials Today: Proceedings* 2020, 33, 2470–2473, doi:10.1016/j.matpr.2020.01.338.
14. Levasseur, D.; Mjejri, I.; Rolland, T.; Rougier, A. Color Tuning by Oxide Addition in PEDOT:PSS-Based Electrochromic Devices. *Polymers* 2019, 11, 179, doi:10.3390/polym11010179.
15. Futsch, R.; Mjejri, I.; Rakotozafy, H.; Rougier, A. PEDOT:PSS-V<sub>2</sub>O<sub>5</sub> Hybrid for Color Adjustment in Electrochromic Systems. *Front. Mater.* 2020, 7, 78, doi:10.3389/fmats.2020.00078.
16. Thakur, V.K.; Ding, G.; Ma, J.; Lee, P.S.; Lu, X. Hybrid Materials and Polymer Electrolytes for Electrochromic Device Applications. *Adv. Mater.* 2012, 24, 4071–4096, doi:10.1002/adma.201200213.
17. Smitha, B.; Sridhar, S.; Khan, A.A. Solid Polymer Electrolyte Membranes for Fuel Cell Applications—a Review. *Journal of Membrane Science* 2005, 259, 10–26, doi:10.1016/j.memsci.2005.01.035.
18. Su'ait, M.S.; Rahman, M.Y.A.; Ahmad, A. Review on Polymer Electrolyte in Dye-Sensitized Solar Cells (DSSCs). *Solar Energy* 2015, 115, 452–470, doi:10.1016/j.solener.2015.02.043.
19. Kwang-Sun, J.; Hee-Soo, M.; Jong-Wook, K.; Jong-Wan, P. Role of Functional Nano-Sized Inorganic Fillers in Poly(Ethylene) Oxide-Based Polymer Electrolytes. *Journal of Power Sources* 2003, 117, 124–130, doi:10.1016/S0378-7753(03)00159-9.

20. Golodnitsky, D.; Ardel, G.; Strauss, E.; Peled, E.; Lareah, Y.; Rosenberg, Y. Conduction Mechanisms in Concentrated LiI-Polyethylene Oxide-  $\text{Al}_2\text{O}_3$ -Based Solid Electrolytes. *J. Electrochem. Soc.* 1997, 144, 3484, doi:10.1149/1.1838037.
21. Forsyth, M. The Effect of Nano-Particle  $\text{TiO}_2$  Fillers on Structure and Transport in Polymer Electrolytes. *Solid State Ionics* 2002, 147, 203–211, doi:10.1016/S0167-2738(02)00017-6.
22. Liu, Y.; Lee, J.Y.; Hong, L. *In Situ* Preparation of Poly(Ethylene Oxide)– $\text{SiO}_2$  Composite Polymer Electrolytes. *Journal of Power Sources* 2004, 129, 303–311, doi:10.1016/j.jpowsour.2003.11.026.
23. Sun, H.Y.; Takeda, Y.; Imanishi, N.; Yamamoto, O.; Sohn, H.-J. Ferroelectric Materials as a Ceramic Filler in Solid Composite Polyethylene Oxide-Based Electrolytes. *J. Electrochem. Soc.* 2000, 147, 2462, doi:10.1149/1.1393554.
24. Albery, W.J.; Chen, Z.; Horrocks, B.J.; Mount, A.R.; Bloor, D.; Monkman, A.T.; Elliot, C.M.; Devreux, F.; Lett, E.; Hillman, A.R.; et al. Electrochemical Properties of Polyethylene Oxide- $\text{Li}[(\text{CF}_3\text{SO}_2)_2\text{N}]\text{-Gamma-LiAlO}_2$  Composite Polymer Electrolytes. 1995, 142, 2118.
25. Manuel Stephan, A. Review on Gel Polymer Electrolytes for Lithium Batteries. *European Polymer Journal* 2006, 42, 21–42, doi:10.1016/j.eurpolymj.2005.09.017.
26. Yun-Sheng, Y.; John, R.; Bing-Joe, H. Ionic Liquid Polymer Electrolytes. *J. Mater. Chem. A* 2013, 1, 2719–2743, doi:10.1039/C2TA00126H.
27. Chand, N.; Rai, N.; Agrawal, S.L.; Patel, S.K. Morphology, Thermal, Electrical and Electrochemical Stability of Nano Aluminium-Oxide-Filled Polyvinyl Alcohol Composite Gel Electrolyte. *Bull Mater Sci* 2011, 34, 1297–1304, doi:10.1007/s12034-011-0318-7.
28. Kurc, B. Gel Electrolytes Based on Poly(Acrylonitrile)/Sulpholane with Hybrid  $\text{TiO}_2/\text{SiO}_2$  Filler for Advanced Lithium Polymer Batteries. *Electrochimica Acta* 2014, 125, 415–420, doi:10.1016/j.electacta.2014.01.117.
29. Yoon-Sung, L.; Seo Hee, J.; Jae-Hong, K.; Seung Sik, H.; Jae-Man, C.; Sun, Y.-K.; Kim, H.; Scrosati, B.; Kim, D.-W. Composite Gel Polymer Electrolytes Containing Core-Shell Structured  $\text{SiO}_2(\text{Li}^+)$  Particles for Lithium-Ion Polymer Batteries. *Electrochemistry Communications* 2012, 17, 18–21, doi:10.1016/j.elecom.2012.01.008.

30. Zhu, Y.; Otle, M.T.; Zhang, X.; Li, M.; Asemota, C.; Li, G.; Invernale, M.A.; Sotzing, G.A. Polyelectrolytes Exceeding ITO Flexibility in Electrochromic Devices. *J. Mater. Chem. C* 2014, 2, 9874–9881, doi:10.1039/C4TC01855A.
31. Verge, P.; Mallouki, M.; Beouch, L.; Aubert, P.H.; Vidal, F.; Tran-Van, F.; Teyssié, D.; Chevrot, C. Electroactive Polymers with Semi-IPN Architectures for Electrochromic Devices. *Molecular Crystals and Liquid Crystals* 2010, 522, 53/[353]-60/[360], doi:10.1080/15421401003726980.
32. Liao, C.; Sun, X.-G.; Dai, S. Crosslinked Gel Polymer Electrolytes Based on Polyethylene Glycol Methacrylate and Ionic Liquid for Lithium Ion Battery Applications. *Electrochimica Acta* 2013, 87, 889–894, doi:10.1016/j.electacta.2012.10.027.
33. Vidal, F.; Plesse, C.; Teyssié, D.; Chevrot, C. Long-Life Air Working Conducting Semi-IPN/Ionic Liquid Based Actuator. *Synthetic Metals* 2004, 142, 287–291, doi:10.1016/j.synthmet.2003.10.005.
34. Kumar, K.V.A.; Chandana, L.; Ghosal, P.; Subrahmanyam, Ch. Simultaneous Photocatalytic Degradation of p -Cresol and Cr (VI) by Metal Oxides Supported Reduced Graphene Oxide. *Molecular Catalysis* 2018, 451, 87–95, doi:10.1016/j.mcat.2017.11.014.
35. Jiménez Reinoso, J.; Leret, P.; Álvarez-Docio, C.M.; del Campo, A.; Fernández, J.F. Enhancement of UV Absorption Behavior in ZnO–TiO<sub>2</sub> Composites. *Boletín de la Sociedad Española de Cerámica y Vidrio* 2016, 55, 55–62, doi:10.1016/j.bsecv.2016.01.004.
36. Huang, R.; Liang, R.; Fan, H.; Ying, S.; Wu, L.; Wang, X.; Yan, G. Enhanced Photocatalytic Fuel Denitrification over TiO<sub>2</sub>/α-Fe<sub>2</sub>O<sub>3</sub> Nanocomposites under Visible Light Irradiation. *Sci Rep* 2017, 7, 7858, doi:10.1038/s41598-017-08439-3.
37. Hergert, H.L.; Kurth, E.F. The Infrared Spectra of Lignin and Related Compounds. I. Characteristic Carbonyl and Hydroxyl Frequencies of Some Flavanones, Flavones, Chalcones and Acetophenones 1. *J. Am. Chem. Soc.* 1953, 75, 1622–1625, doi:10.1021/ja01103a031
38. Sung, J.; Lee, D.G.; Lee, S.; Park, J.; Jung, H.W. Crosslinking Dynamics and Gelation Characteristics of Photo- and Thermally Polymerized Poly(Ethylene Glycol) Hydrogels. *Materials* 2020, 13, 3277, doi:10.3390/ma13153277.



## Captions

Table 1 : Deposition parameter of  $\text{WO}_3$  and  $\text{V}_2\text{O}_5$  films on ITO coated glass substrates

Table 2 : Switching time of oxidative reaction for electrochromic symmetrical displays built from PEDOT:PSS and different colored electrolytes when a potential of +1.5 V is applied. Potentials of +1.5 V and -1.5 V were applied for 30 s alternatively during 500 cycles.

Table 3 : Values of the chromaticity parameters  $L^*$ ,  $a^*$  and  $b^*$  and optical contrast  $\Delta E^*$ . 1<sup>st</sup> cycle reduced and oxidized, neutral and electrolyte values correspond to the photographs on figure 5. Values for 500<sup>th</sup> were obtained measuring the displays colors after 500 CA cycles of +1.5 V 30 s and -1.5V 30 s.

Table 4 : Colorimetric parameters and optical contrasts of the  $\text{WO}_3/\text{electrolyte}/\text{Li}_x\text{V}_2\text{O}_5$  display shown on figure 7.

Table 5 : Optical contrasts between patterns of the reduced and oxidized states of  $\text{WO}_3/\text{electrolyte}/\text{Li}_x\text{V}_2\text{O}_5$  display.

## Figures Captions :

Figure 1 : Photographs and values of the chromaticity parameters  $L^*$ ,  $a^*$  and  $b^*$  of the electrolytes sandwiched between two glass substrates in respect of the addition of White, Yellow, Red and Green pigments.

Figure 2 : Electrolyte ionic conductivity measurements at 40 °C in the frequency range from 100 KHz to 10Hz with perturbation amplitude of 10 mV by varying : a) Titanium oxide ( $\text{TiO}_2$ ) quantity (wt% of the electrolyte); b) Color with the same formulations as those presented in figure 1.

Figure 3 : FT-IR intensity datas for the colorless electrolyte before thermal treatment and for the colorless and colored electrolytes after thermal treatment.

Figure 4 : 1<sup>st</sup> (a) and 500<sup>th</sup> (b) oxidative chronoamperograms (CA) of the electrochromic symmetrical displays built from PEDOT:PSS with different colored electrolytes. Potentials of +1.5 V and -1.5 V were applied for 30 s alternatively during 500 cycles.

Figure 5 : Photographs of electrolytes and electrochromic symmetrical displays built from PEDOT:PSS and electrolytes with different pigments. Reduced and oxidized states are obtained when a potential of -1.5 V and respectively +1.5 V are applied to the electrode. Neutral state is obtained after applying an initial potential of -1.5 V and 1 hour of open circuit voltage. The electrolyte was sandwiched between two glass substrates to obtain the electrolyte photographs.

Figure 6 : Capacity percentages of electrochromic symmetrical displays built from PEDOT:PSS using different colored electrolytes when a potential of +1.5 V is applied. Potentials of +1.5 V and -1.5 V were applied for 30 s alternatively during 500 cycles.

Figure 7 : Photographs of the multicolored  $\text{WO}_3/\text{electrolyte}/\text{Li}_x\text{V}_2\text{O}_5$  display with four colored electrolytes. a) A potential of -1.5 V is applied showing a reduced state. b) A potential of +1.5 V is applied showing an oxidized state.

Target	Power source	Power (W)	Pressure (Pa)	Ar : O <sub>2</sub> (sccm)	Deposition rate (nm/m)	Thickness (± 20 nm)
WO <sub>3</sub>	RF	75	2	49:1	6.8	340
V	RF	200	2	45:5	1.75	210

**Table 1**

	<b>Colorless</b>	<b>White</b>	<b>Yellow</b>	<b>Red</b>	<b>Green</b>
<b>Cycle 1 (s)</b>	0.36	0.33	0.34	0.41	0.37
<b>Cycle 500 (s)</b>	0.34	0.33	0.36	0.40	0.36

**Table 2**

		<i>1<sup>st</sup> cycle</i>			<i>500<sup>th</sup> cycle</i>			Neutral	Electrolyte
		Reduced	Oxidized	$\Delta E^*$	Reduced	Oxidized	$\Delta E^*$		
<b>White</b>	L*	38.9	59.6		38.7	59.3		57.5	80.5
	a*	-1.9	-3.6	<b>29.4</b>	-3.4	-3.5	<b>26.7</b>	-3.8	-1.2
	b*	-28.7	-7.9		-25.0	-7.9		-8.0	0.1
<b>Yellow</b>	L*	24.7	37.0		26.9	38.6		36.1	49.8
	a*	3.5	10.2	<b>21.7</b>	2.3	9.3	<b>21.5</b>	9.1	16.7
	b*	24.5	41.0		21.3	38.0		39.6	54.4
<b>Red</b>	L*	19.5	27.3		18.1	28.4		25.3	35.2
	a*	11.0	21.3	<b>18.5</b>	11.0	21.7	<b>19.8</b>	19.8	29.3
	b*	0.7	13.9		0.9	13.9		12.7	21.8
<b>Green</b>	L*	33.3	53.4		33.6	53.4		50.1	67.6
	a*	-10.6	-13.9	<b>25.0</b>	-11.5	-13.1	<b>26.2</b>	-13.6	-18.1
	b*	-15.1	-0.5		-16.8	0.3		-1.5	10.1

**Table 3**

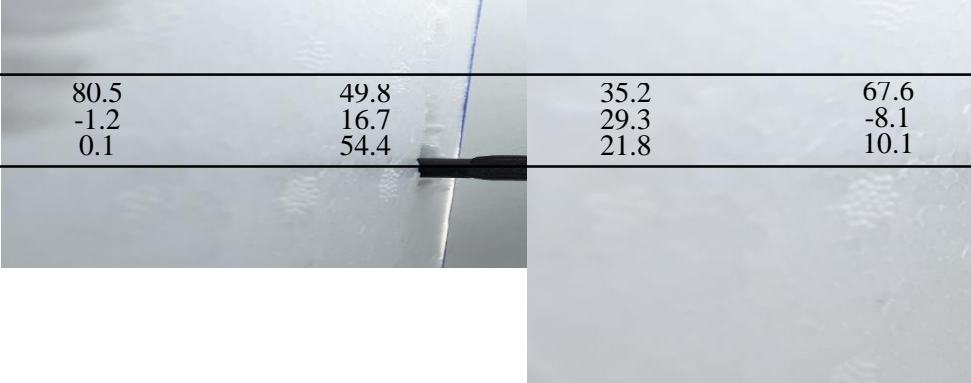
	Reduced			Oxidized			$\Delta E^*$
	L*	a*	b*	L*	a*	b*	
<b>White</b>	8.8	5.4	-19.7	72.9	-3.5	1.3	68.0
<b>Yellow</b>	9.3	1.9	-13.7	69.0	-0.1	19.6	68.4
<b>Red</b>	9.7	3.2	-14.2	64.1	6.1	8.5	59
<b>Green</b>	11.6	3.2	-15.6	70.0	-8.3	3.9	62.6

**Table 4**

		<b>White/ Yellow</b>	<b>White/ Red</b>	<b>White/ Green</b>	<b>Yellow/ Red</b>	<b>Yellow/ Green</b>	<b>Red/ Green</b>
<b>Contrast be- tween patterns</b>	<b>Reduced</b>	7.0	6.0	5.4	1.4	3.3	2.4
	<b>Oxidized</b>	19.0	14.8	6.2	13.6	17.7	16.2

**Table 5**

	White	Yellow	Red	Green
L*	80.5	49.8	35.2	67.6
a*	-1.2	16.7	29.3	-8.1
b*	0.1	54.4	21.8	10.1



**Figure 1**



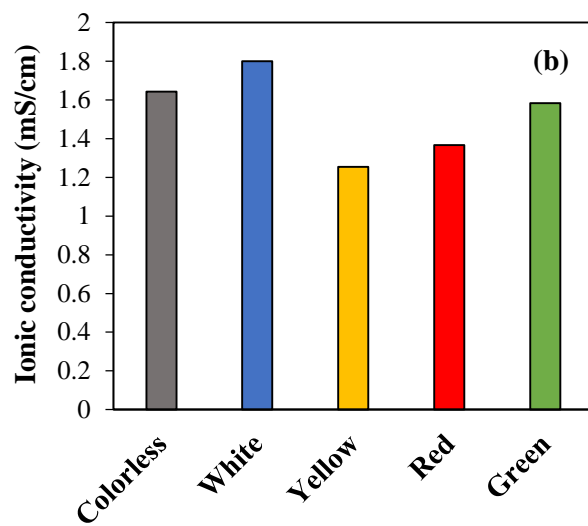
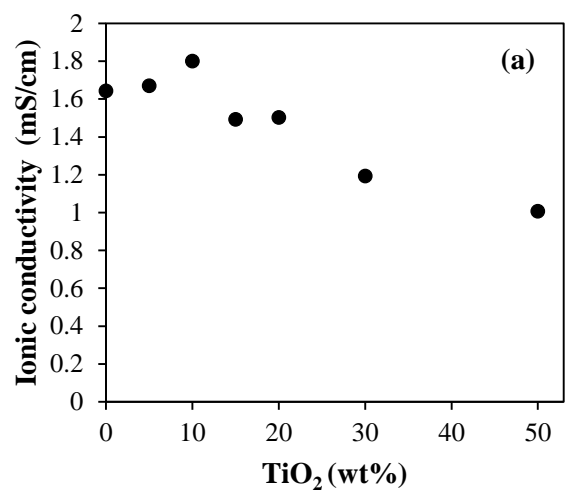
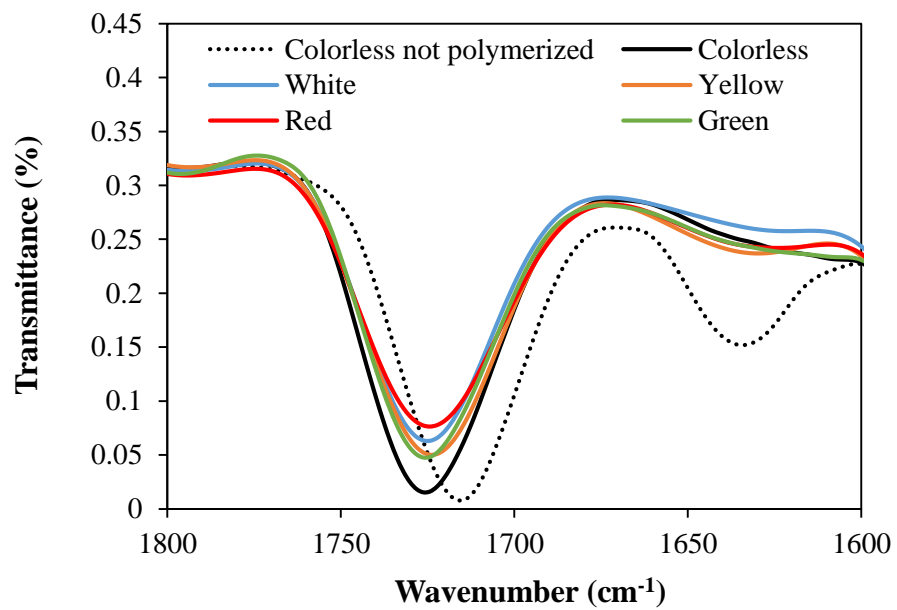


Figure 2



**Figure 3**

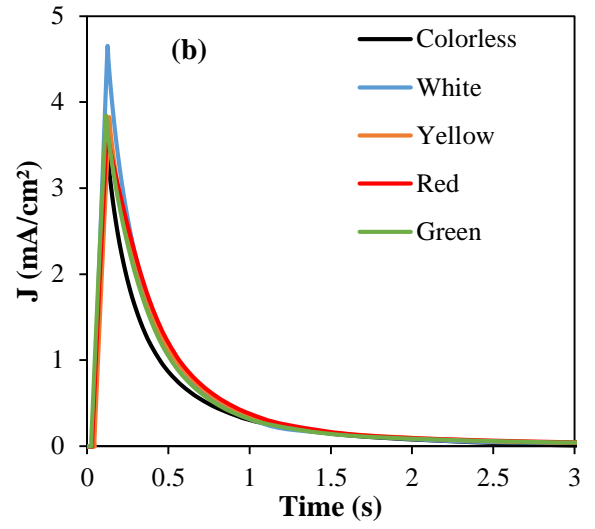
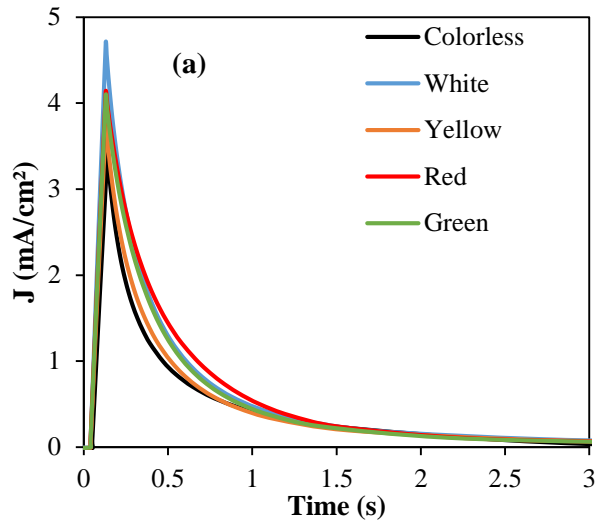


Figure 4




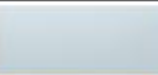





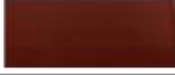
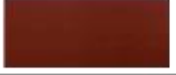





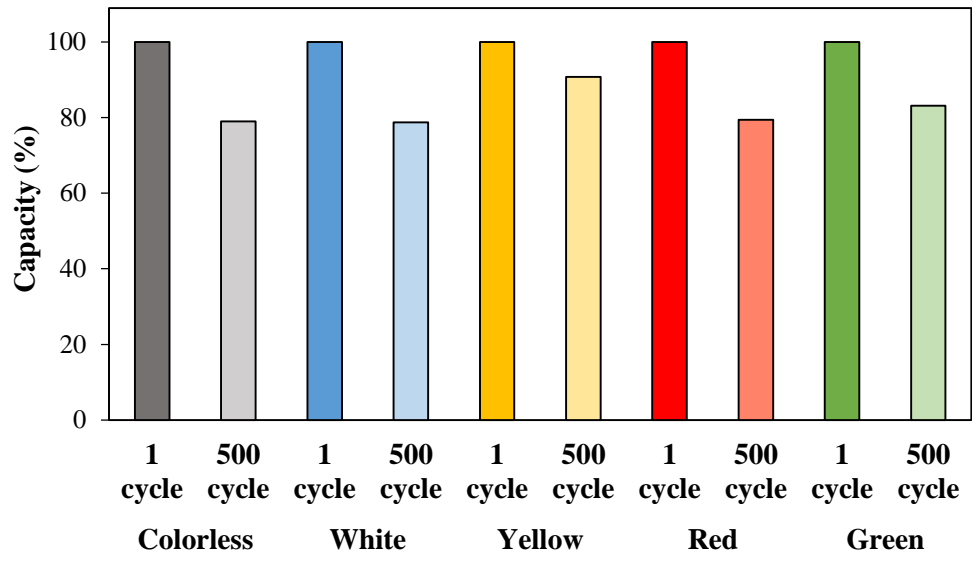
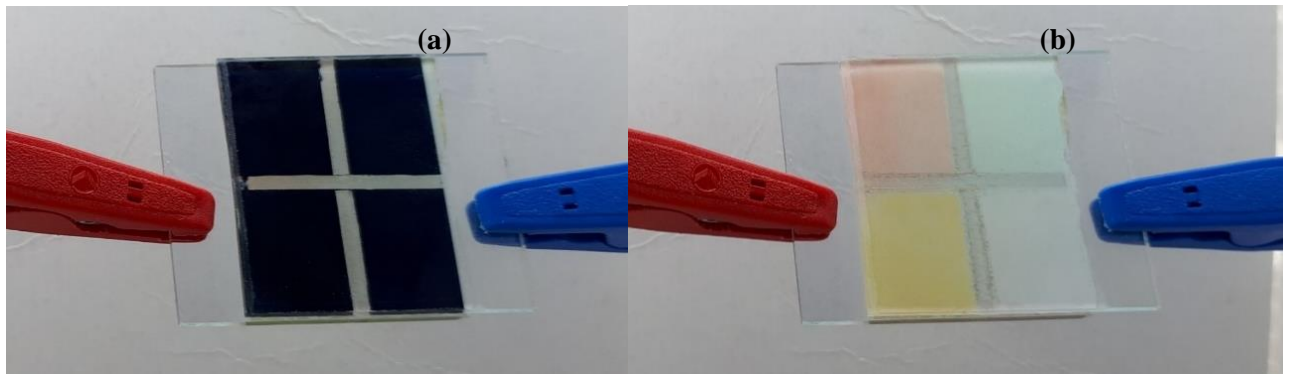
	Reduced	Oxidized	Neutral	Electrolyte
White				
Yellow				
Red				
Green				

Figure 5



**Figure 6**



**Figure 7**